Orbital effects in the inelastic magnetic scattering of x rays

D. Kechrakos, K. N. Trohidou, and S. Taddei
Institute of Materials Science, National Centre for Scientific Research ''Demokritos,'' 15310 Athens, Greece
(Received 12 February 1997; revised manuscript received 9 June 1997)

The cross section for the inelastic scattering of circularly polarized x rays from a spin-polarized electron, bound to a hydrogen atom, is calculated using the exact final electron wave function. In the total amplitude, charge and spin scattering are treated to first order and orbital effects to second order in perturbation theory for the vector potential of the photon field. The matrix element for orbital scattering is calculated with two methods: (a) the exact calculation in second-order perturbation theory using Green's function techniques, (b) the quasielastic approximation. The validity of the latter is discussed. It is shown that as the energy transfer to the atomic system increases the orbital effects decrease relative to spin effects in the magnetically scattered intensity. For large energy transfers compared to the electron binding energy (Compton limit) the orbital effects are approximately two to three orders of magnitude smaller than their spin counterparts. Our results are in agreement with recent experiments. [S0163-1829(97)02442-9]

The possibility of experimental determination of the spin-polarized momentum distribution in solids by means of Compton scattering of circularly polarized x-rays has been predicted[1] a long time ago and subsequent measurements[2] have verified this prediction. Furthermore, the possibility of separating the spin and the orbital contributions to the magnetization density by exploiting the photon polarization effects was theoretically analyzed and experimentally demonstrated in early magnetic diffraction experiments.[3]

However, the Bragg condition that governs a diffraction process imposes restrictions on the scattering geometry to be implemented in an experiment and could also make the detection of the magnetically scattered intensity practically impossible. This is, for example, the case of simple ferromagnets like Fe, where magnetic reflections are hidden under the superimposed strong charge reflections. Thus, in practical terms, the detection of magnetic peaks is possible for systems where the crystallographic and magnetic structures are different, as is the case of antiferromagnets like Ho.[3,4] For a ferromagnetic material, the magnetic contribution to the scattered signal can be isolated by use of circular polarization in the primary beam, which induces an interference between the charge and magnetic contributions to the cross section. The latter can be modulated in sign by either reversing the helicity of the primary beam or by reversing the net magnetic moment of the sample by application of an external magnetic field.

On the other hand, in an inelastic-scattering process, the Bragg condition is not present and the momentum transfer is determined by the choice of the energy of the incident photon beam and the angle of scattering. A variation of these two parameters could in principle lead to observable magnetic effects, away from any diffraction peak. This idea motivated recent Compton measurements of magnetization in ferromagnetic iron and cobalt.[5] Despite the fact that in these materials the orbital magnetization density is about one to two orders of magnitude less than the spin counterpart, the results of this work[5] indicated that both the magnetic components could be measured. However, more detailed experiments by the same group of scientists,[6] on $HoFe_3$, which has a dominant orbital magnetization, clearly demonstrated that the orbital magnetic density is not detectable in a conventional Compton experiment. Theoretical support to the latter experimental findings was given on the basis of the impulse approximation (IA), that predicts identically zero orbital magnetic intensity.[7–9]

In the spirit of the IA one refers to large primary photon energies and assumes that the energy transfer to the target is large compared to the electron binding energy. Consequently, the initial and final electron states are plane waves, to a good approximation, and the momentum of the electron-photon system is conserved. While very appealing on the grounds of physical intuition, the theoretical approximations involved in the IA merit a more careful examination with respect to whether they correspond to the actual experimental conditions. In a previous work[8] first-order corrections to the IA for orbital scattering have been estimated of the order of the ratio $(E_b/\hbar\omega)$, where E_b is the electron binding energy and $\hbar\omega$ the energy transfer.

The recent experiments[6] with hard x-rays add weight to the case to examine in detail a well-defined and realistic model of the Compton scattering by an unpaired bound electron. The purpose of our present work is to provide a quantitative estimate of the orbital effects in the inelastic process by performing an *exact* numerical calculation for a model system. Our calculation is exact in two aspects: (i) the final electron state is the Coulomb continuum wave function, and (ii) the matrix element for orbital scattering is given by the Kramers-Heisenberg dispersion formula. Therefore, both the validity of the IA is tested and the assumption usually made in Compton scattering that it is mildly inelastic.

As a model system we have chosen a hydrogen atom in the $2p$ state. Since we are mainly interested in high-energy photons (>10 keV) the photon wavelength is of the order of the Bohr radius ($\lambda<1.2$ Å) and, consequently, scattering events from different atoms are to a good approximation incoherent.[7] Furthermore, many electron effects within the same atom can be incorporated in a more realistic single-electron atomic potential. Therefore the choice of a single-electron system as a model is justified.

We consider a photon of energy ω_1 wave vector $\mathbf{k}_1$, and polarization $\hat{\varepsilon}_1$ that is scattered off the atomic electron with

energy E_1. The secondary photon has energy ω_2, momentum $\mathbf{k}_2$, and polarization $\hat{\varepsilon}_2$, while the electron is scattered into a state in the continuum with energy E_2 and momentum $\mathbf{p}$. The differential cross section for this event is given by Fermi's Golden Rule

$$\left.\frac{d^3\sigma}{d\omega d\Omega d\Omega'}\right|_{1\to 2} = r_e^2\left(\frac{\omega_2}{\omega_1}\right)\cdot|\langle 2|M|1\rangle|^2\cdot\delta(E_1-E_2+\omega_1-\omega_2), \tag{1}$$

where, r_e is the classical electron radius. The total transition operator M (Refs. 10 and 11) is a linear combination of charge (M_{C}), orbital (M_{O}), and spin (M_{S}) amplitudes. The charge scattering is given by the Thomson term

$$M_{\mathrm{C}} = e^{i(\mathbf{k}_1-\mathbf{k}_2)\cdot\mathbf{r}}(\hat{\varepsilon}_2\cdot\hat{\varepsilon}_1). \tag{2a}$$

The orbital term is described by the well-known Kramers-Heisenberg dispersion formula

$$M_{\mathrm{O}} = -\frac{1}{m_e}\sum_{\nu}\left\{\begin{array}{c} e^{-i\mathbf{k}_2\cdot\mathbf{r}}(\hat{\varepsilon}_2\cdot\mathbf{p})|\nu\rangle(E_\nu-E_1-\omega_1+i\varepsilon)^{-1}\langle\nu|e^{i\mathbf{k}_1\cdot\mathbf{r}}(\hat{\varepsilon}_1\cdot\mathbf{p})+ \\ e^{i\mathbf{k}_1\cdot\mathbf{r}}(\hat{\varepsilon}_1\cdot\mathbf{p})|\nu\rangle(E_\nu-E_1+\omega_2)^{-1}\langle\nu|e^{-i\mathbf{k}_2\cdot\mathbf{r}}(\hat{\varepsilon}_2\cdot\mathbf{p}) \end{array}\right\}, \tag{2b}$$

Finally, for the spin term we use an approximate expression that is valid for high photon energies relatively to the electron binding energy[10]

$$M_{\mathrm{S}} = -i\left(\frac{\omega_1}{m_e}\right)e^{i(\mathbf{k}_1-\mathbf{k}_2)\cdot\mathbf{r}}\mathbf{S}\cdot\mathbf{B}, \tag{2c}$$

where $\mathbf{S}$ is the electron spin, m_e the electron rest mass, and $\mathbf{B}$ the polarization factor[1,7]

$$\mathbf{B} = (\hat{\varepsilon}_2\times\hat{\varepsilon}_1)+(\hat{k}_1\times\hat{\varepsilon}_1)\times(\hat{k}_2\times\hat{\varepsilon}_2)+(\hat{k}_2\times\hat{\varepsilon}_2)\cdot(\hat{k}_2\cdot\hat{\varepsilon}_1) - (\hat{k}_1\times\hat{\varepsilon}_1)\cdot(\hat{k}_1\cdot\hat{\varepsilon}_2). \tag{2d}$$

The first term in Eq. (2d) comes from the first-order term in the perturbation expansion for the vector potential of the electromagnetic field. To obtain the last three terms in Eq. (2d) the vector potential is treated in second-order perturbation theory and the limit of high photon energy relative to the electron binding energy is assumed ($\omega_1/|E_1|\gg 1$). The validity of the latter approximation for spin scattering is not discussed in this work. Natural units $\hbar=c=1$ are used in Eq. (2) and further on.

The full calculation of the orbital term, Eq. (2b), involves the sum over intermediate states, labeled by ν. that it is quite cumbersome. However, for *elastic* scattering of photons with energy much higher than any atomic resonance ($\omega_1,\omega_2 \gg|E_1|$), the orbital amplitude in Eq. (2b) tends to the limiting value[10]

$$\mathbf{Z}(k_1,k_2)\cdot(\hat{\epsilon}_2\times\hat{\epsilon}_1) = -i\left(\frac{\omega_1}{m_e}\right)\frac{i}{k_1^2}\,e^{i\mathbf{k}\cdot\mathbf{r}}(\mathbf{k}\times\mathbf{p})\cdot(\hat{\varepsilon}_2\times\hat{\varepsilon}_1), \tag{3}$$

where $\mathbf{k}=\mathbf{k}_1-\mathbf{k}_2$ is the momentum transfer. Despite the fact that the approximations involved in Eq. (3) are strictly valid for elastic scattering, it has been argued[5,6] that Eq. (3) describes correctly the orbital effects in a Compton scattering process, because the latter is only *mildly* inelastic, i.e., $\omega_1\sim\omega_2$. We refer to Eq. (3) as the quasielastic approximation (QA) to the orbital amplitude. The validity of the QA in the interpretation of Compton scattering events is discussed below.

In a Compton scattering experiment the polarization of the secondary photon beam as well as the direction of the ejected electron are not recorded.[5,6] Consequently, Eq. (1) is first integrated over the final photon polarization $\hat{\varepsilon}_2$ and the photon polarization density matrix[7,12] for the primary photon beam is introduced. Second, an average over the final electron direction and spin polarization is performed. The resulting double differential cross section is written in the form

$$\frac{d^2\sigma}{d\omega_2 d\Omega_2} = S_{\mathrm{C}}+S_{\mathrm{CS}}+S_{\mathrm{CO}}+O(\tau^3). \tag{4}$$

Magnetic effects, to leading order in $\tau=(\omega_1/m_e)$, are described by the interference cross sections between charge-orbital (S_{CO}) and charge-spin amplitudes (S_{CS}). The interference terms are nonvanishing when the photon beam is circularly polarized. Polarization analysis of the double differential cross section has shown[7] that both these terms have the form $S_{\mathrm{IF}}=a+P_2 b$, where P_2 is the mean helicity of the primary beam, while the charge cross section is independent of P_2. Thus, reversing the primary beam polarization and subtracting the corresponding spectra, one obtains the asymmetric cross section, defined by

$$S_{\mathrm{A}} = [S_{\mathrm{CS}}^{(+)}-S_{\mathrm{CS}}^{(-)}]+[S_{\mathrm{CO}}^{(+)}-S_{\mathrm{CO}}^{(-)}]\equiv S_{\mathrm{ACS}}+S_{\mathrm{ACO}}, \tag{5}$$

which does not contain the undesired charge term S_{C}. Thus magnetic effects can be extracted from the spectrum. Experimentally, the asymmetric cross section can be measured by reversing the magnetization of the sample with the aid of an external field, which is in principle equivalent to reversing the polarization of the beam. The central problem is therefore the computation of the asymmetric cross sections, Eq. (5), for charge-orbital and charge-spin scattering.

In the present calculation, the charge-orbital asymmetric cross section has been calculated using two schemes: (i) the full orbital amplitude, Eq. (2b), and (ii) the quasielastic or-

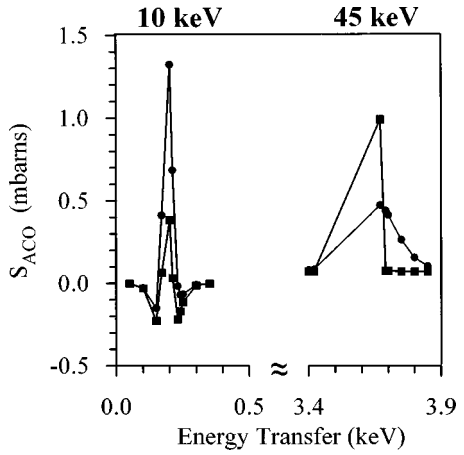

FIG. 1. Comparison of the quasielastic approximation with the exact theory for orbital scattering of 10 and 45 keV beams. (●) Quasielastic approximation, (■) exact theory. The lines serve only as a guide to the eye. Scattering geometry: incoming beam along the magnetization axis, outgoing beam perpendicular to the magnetization axis. Circular polarization of primary beam: 100%.

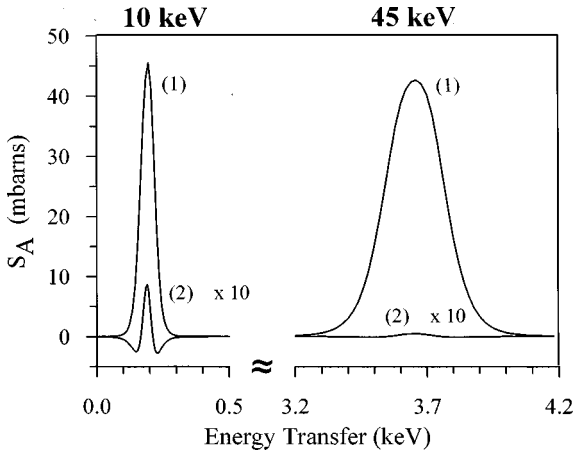

FIG. 2. Comparison of orbital and spin scattered intensities of 10 and 45 keV beams. (1) Spin scattering intensity. (2) Orbital scattering intensity, magnified by a factor of 10. Scattering geometry: incoming beam perpendicular to the magnetization axis, outgoing beam along the magnetization axis. Circular polarization of primary beam: 100%.

bital amplitude, Eq. (3). The main ingredients of the calculation procedure are the following: The initial and final electron states have been expressed in momentum space. For the continuum state a contour integral representation has been used.[13] The momentum space integrations required for the charge matrix element, Eq. (2a), the spin matrix element, Eq. (2c), and the approximate orbital matrix element, Eq. (3), have been done analytically using expressions for a general two-denominator integral.[14] The calculation of the full orbital matrix element, Eq. (2b), has been done along the lines of Ref. 13, extended to the case of the $2p$-electron state. The final result for the matrix element was expressed in terms of hypergeometric functions of four variables (Lauricella functions) that were expanded in power series and were computed numerically. Analytic continuation schemes[13] were used to ensure convergence of the series.

In the numerical results presented below, we constantly assumed that the electron is initially at the $2p$ state of a hydrogen atom ($E_1 = -3.4$ eV) with initial spin-polarization and orbital angular momentum along the positive z axis ($s_z = +\frac{1}{2}$, $m_z = +1$). The primary photon beam is 100% circularly polarized ($P_2 = \pm 1$).

First, we compare the predictions of the exact perturbation scheme for orbital scattering, Eq. (2b), with those of the quasielastic approximation, Eq. (3). In Fig. 1 we plot the orbital part of the asymmetric cross section (S_{ACO}) for primary photon beams with energy 10 and 45 keV. In the scattering geometry assumed in Fig. 1, the incoming photon beam is along the magnetization axis (z axis) and the outgoing beam perpendicular to the magnetization axis. This geometry is known to maximize orbital effects, while spin scattering is absent.[5,6] Both curves exhibit the well-known sharp peak around the (free) electron recoil energy (ω_0), given as

$$\omega_0 = \omega_1(1-\cos\theta) + m - \sqrt{m^2 + 2m\omega_1(1-\cos\theta) - \omega_1^2 \sin^2\theta}, \tag{6}$$

where θ is the scattering angle. The calculation using the full expression is extremely time consuming, because in the region of the Compton peak the Lauricella function arguments cross their circle of convergence, and the analytic continuation schemes converge very slowly. Therefore only a few indicative points are shown. Notice in Fig. 1 that as the primary energy increases, the predictions of the QA deviate from the exact result. We attribute this feature to the increasing inelastic character of the process. In particular, the energy loss of the 10 kev primary beam is approximately 2%, while for the 45 keV beam this is increased to approximately 8%. However, for photon energies in the range $10\text{ keV} < \omega_1 < 45\text{ keV}$, the predictions of the two calculations agree within an order of magnitude. Therefore, the quasielastic approximation describes adequately the orbital contributions to the magnetic intensity.

In order to estimate the importance of orbital effects with respect to their spin counterpart, we choose next a scattering

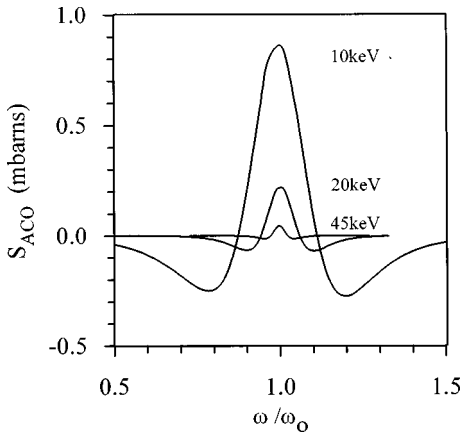

FIG. 3. Decay of orbital effects with incident photon energy. The horizontal axis is the ratio of the energy transfer to the atomic electron (ω) over the recoil energy of a free electron (ω_0). Scattering geometry: incoming beam perpendicular to the magnetization axis, outgoing beam along the magnetization axis. Circular polarization of primary beam: 100%.

geometry in which both contributions are present. In particular, the incoming beam is perpendicular to the magnetization axis and the outgoing beam is along the magnetization axis.[5,6] In Fig. 2 the line shapes for orbital and spin scattering are shown for a 10 and a 45 keV beam. By comparison of the peak values we can conclude that the orbital contribution is smaller than the spin contribution by a factor of 10^2-10^3. This result supports the conclusions reached in recent Compton measurements[6] about the smallness of the orbital term.

To demonstrate the gradual disappearance of the orbital effects as the primary photon energy is increased, we have plotted in Fig. 3 the orbital part of the asymmetric cross section for beam energies of 10, 20, and 45 keV and for the same scattering geometry as in Fig. 2. At this point, we wish to make a connection with the IA that predicts identically zero orbital intensity. In particular, the height of the orbital peaks in Fig. 3 could be thought of as corrections to the IA up to all orders in the electron binding energy. From this figure we conclude that for photon beams with energy of a few tens of keV, the orbital intensity is vanishingly small ($10^{-3}-10^{-6}$ b) and the impulse approximation regime is reached.

In conclusion, we have used a hydrogen atom and an exact calculation method to study the magnetic intensity of inelastically scattered hard x rays. The description of the Compton process as mildly inelastic was shown to be a reasonable approximation for photon energies in the range 10–45 keV. In the same energy range orbital effects in the magnetic intensity were found to be approximately two to three orders of magnitude smaller than spin effects, therefore the prediction of the IA that orbital effects are not present is satisfactory. Extensions of the calculation to *d* or *f* electrons, that are responsible for the magnetic properties of solids, are not expected to modify qualitatively the above picture.

We would like to thank S. W. Lovesey for many useful discussions. This work has been supported by the Human Capital and Mobility Project No. CHRX-CT930135.

[1] P. M. Platzman and N. Tzoar, Phys. Rev. B **2**, 3556 (1970).
[2] N. Sakai and K. Ono, Phys. Rev. Lett. **37**, 351 (1976).
[3] F. de Bergevin and M. Brunel, Acta Crystallogr., Sect. A **37**, 314 (1981); **37**, 324 (1981); in *Structure and Dynamics of Molecular Systems*, edited by R. Daudel *et al.* (Reidel, Dordrecht, 1986), Vol. 2, p. 69.
[4] D. Gibbs, D. R. Harshman, E. D. Isaacs, D. B. McWhan, D. Mills, and C. Vettier, Phys. Rev. Lett. **61**, 12 417 (1988).
[5] S. P. Collins, M. I. Cooper, S. W. Lovesey, and D. Laundy, J. Phys. Condens. Matter **2**, 6439 (1990).
[6] M. J. Cooper, E. Zukowski, S. P. Collins, T. N. Timms, F. Itoh, and H. Sakurai, J. Phys. Condens. Matter **4**, L399 (1992).
[7] S. W. Lovesey, Rep. Prog. Phys. **56**, 257 (1993).
[8] P. Carra, M. Fabrizio, G. Santoro, and B. Thole, Phys. Rev. B **53**, R5994 (1996).
[9] S. W. Lovesey, J. Phys. Condens. Matter **8**, L353 (1996).
[10] M. Blume, J. Appl. Phys. **57**, 3615 (1985).
[11] H. Grotch, E. Kazes, G. Bhatt, and D. A. Owen, Phys. Rev. A **27**, 243 (1983).
[12] M. Blume and D. Gibbs, Phys. Rev. B **37**, 1779 (1988).
[13] M. Gavrila, Phys. Rev. A **6**, 1348 (1972).
[14] R. R. Lewis, Phys. Rev. **102**, 537 (1956).